Published in final edited form as:
ACS Appl Mater Interfaces. 2010 October ; 2(10): 2749–2758. doi:10.1021/am100616b.

Functionalized Nanoporous Silica for the Removal of Heavy Metals from Biological Systems: Adsorption and Application

Wassana Yantasee[*,†], **Ryan D. Rutledge**[‡], **Wilaiwan Chouyyok**[‡], **Vichaya Sukwarotwat**[‡], **Galya Orr**[‡], **Cynthia L. Warner**[‡], **Marvin G. Warner**[‡], **Glen E. Fryxell**[‡], **Robert J. Wiacek**[‡], **Charles Timchalk**[‡], and **R. Shane Addleman**[*,‡,§]
Department of Biomedical Engineering, OHSU School of Medicine, Portland, Oregon 97239, and Pacific Northwest National Laboratory (PNNL), Richland, Washington 99352

Abstract

Surface-functionalized nanoporous silica, often referred to as self-assembled monolayers on mesoporous supports (SAMMS), has previously demonstrated the ability to serve as very effective heavy metal sorbents in a range of aquatic and environmental systems, suggesting that they may be advantageously utilized for biomedical applications such as chelation therapy. Herein we evaluate surface chemistries for heavy metal capture from biological fluids, various facets of the materials' biocompatibility, and the suitability of these materials as potential therapeutics. Of the materials tested, thiol-functionalized SAMMS proved most capable of removing selected heavy metals from biological solutions (i.e., blood, urine, etc.) Consequentially, thiol-functionalized SAMMS was further analyzed to assess the material's performance under a number of different biologically relevant conditions (i.e., variable pH and ionic strength) to gauge any potentially negative effects resulting from interaction with the sorbent, such as cellular toxicity or the removal of essential minerals. Additionally, cellular uptake studies demonstrated no cell membrane permeation by the silica-based materials generally highlighting their ability to remain cellularly inert and thus nontoxic. The results show that organic ligand functionalized nanoporous silica could be a valuable material for a range of detoxification therapies and potentially other biomedical applications.

Keywords

nanoporous; mesoporous; SAMMS; thiol; iminodiacetic acid; biocompatibility; heavy-metal chelation; sorbent; ion exchange; detoxification

INTRODUCTION

Nanoporous silica provides a material support structure that is hydrothermally stable while retaining enough malleability to allow precise control of the pore morphology and installation of a wide range of surface chemistries. The ability to design and build such functional nanoporous materials from elements (silicon and oxygen) that are not intrinsically toxic is attractive for biomedical applications. Nanoporous silicas are of particular interest

[*]Tel.: 503-418-9306. Fax: 503-418-9311. yantasee@bme.ogi.edu.
[†]OHSU School of Medicine.
[‡]Pacific Northwest National Laboratory.
[§]Tel.: 509-371-6824. Fax: 509-375-2186. shane.addleman@pnl.gov.

Supporting Information Available: Additional experimental detail, metal contact data in "protein-free" matrixes, a cell culture schematic, ionic strength effects on SH-SAMMS metal uptake, and SH-SAMMS kinetic studies and capacity measurements in biological fluids. This material is available free of charge via the Internet at http://pubs.acs.org.

because their high specific surface area provides a very large capacity for the adsorption and desorption of molecular and ionic species (1). Furthermore, the well-ordered porosity enables rapid and controlled release or capture of small molecules (2). The porosity and structure can even be arranged to immobilize biomolecules so that they retain much of their activity (3–8). The flexible surface chemistry and biocompatibility have enabled mesoporous silica materials to be used to facilitate such biologically sensitive processes as gene transfection (9–12). Nanostructured silica doped with dyes has been shown to be valuable for monitoring of various biological processes and even imaging of internal cellular processes (5, 9, 12–20). Controlled drug release from mesoporous materials has been extensively explored (21–33). Modified mesoporous materials have recently been reported for the directed and controlled delivery of anticancer drugs such as titanocene complexes (9, 34–37). In an effort to expand the biomedical applicability of these types of materials, the use of functionalized nanoporous silica as a sorbent for the removal of toxins from biological fluids is explored herein with a specific focus upon the treatment of heavy metal exposure.

Industrial activities have driven the wide-spread refinement and utilization of heavy metals with the unfortunate concurrent releases of these toxic materials into the environment. Heavy metal remediation, detoxification, and assay are of significant interest because exposure to metals like cadmium (Cd), lead (Pb), mercury (Hg), and arsenic (As) are known to cause a range of diseases that are detrimental to human health (38–47). Functionalized nanoporous silica has been shown to enable the rapid diagnosis of heavy metal exposure with inexpensive field-portable instruments (48, 49). Improvements in heavy metal detoxification methods would also be beneficial, and advanced materials may offer a solution.

Presently, the preferred method for the removal of heavy metals from the body involves organic chelators such as ethylenediaminetetraacetic acid (EDTA) and 2,3-dimercaptosuccinic acid (DMSA). However, these methods require multiple applications by medical personnel and may burden and damage the renal system as the metal chelates are cleared from the body. In addition, the chelation agents are known to extract essential metals (i.e. iron, magnesium, calcium, and zinc) from the body, resulting in mineral deficiencies, which can produce a number of detrimental side effects (e.g., anemia due to iron deficiency) (50). Human deaths have recently been reported that were attributed to cardiac arrest resulting from hypocalcemia due to EDTA chelation therapy (51). A treatment administrated orally and providing adsorption from the gastrointestinal tract would limit immediate systemic uptake of the ingested toxic metals and facilitate their fecal elimination. Further, oral administration eliminates the need for medical professionals to be involved in the treatment while enabling convenient and safe use. This mode of treatment would be similar to the oral administration of Prussian blue (insoluble iron ferrocyanide powder), which was approved in 2003 by the Food and Drug Administration (FDA) for the removal of thallium and cesium from the human body (52). A solid-phase sorbent capable of effectively capturing toxic species directly from relevant biological fluids, while ignoring essential metals, would clearly be therapeutically advantageous.

Self-assembled monolayers on mesoporous silica (SAMMS is a registered trademark) has been shown to be a very effective heavy-metal sorbent in aqueous matrixes, outperforming other sorbents such as polymer resins and activated carbon under most conditions (53–55). SAMMS has the advantage of nanoporous silica (high surface area and open porosity) combined with a high-density, covalently bound ligand field enhancing sorbent capacity, affinity, and stability (1, 56, 57). Diverse surface functionality can be installed to adjust the sorbent selectivity for the capture of target materials (58–61). Heavy metal chelation surface chemistries analogous to EDTA and DMSA have been installed and shown to be very

effective SAMMS sorbents (1,54,56,57,62,63). Anionic heavy metals such as chromate and arsenate can also be captured by the installation of cationic transition-metal complexes (64–66). SAMMS success as a sorbent in aquatic media is well-documented and suggests a potential utility in biological systems. However, the shift in applicability from aqueous matrixes encountered in environmental samples to biological fluids is not a trivial matter because of the complex composition of biological fluids (e.g., high protein content, potential cellular interactions, etc.).

Applications needing toxin capture from biological fluids are not limited to heavy metal chelation. A number of situations can be envisioned in which high-efficacy solid-phase sorbents called upon to aid in the removal of toxic species from biological fluids would be therapeutically beneficial. For example, an increase in the use of gadolinium (Gd)-based contrast agents for imaging techniques (i.e., MRI) has been linked to a potentially fatal skin disease, nephrogenic systemic fibrosis, in some patients, and the removal of excess or free Gd from the system should be advantagous (67, 68). Radioisotopes coupled with cancer binding agents are currently being used as a treatment for a range of cancers, and the removal of free radioisotopes not bound to cancerous tissue would significantly reduce systemic side effects or enable increased dosages for equivalent side effects (69–72). Platinum compounds have demonstrated a remarkable effectiveness at fighting a number of cancers but are quite toxic, which limits their dosages and utilization (73–75). Analogous to radioisotopes, the removal of free platinum compounds that did not bind to the cancer could be very beneficial. Direct filtration of toxic metals from blood would enable dialysis-style treatments without placing any burden upon the kidneys (67). Clearly, for many applications, the removal of excess, unbound, or unneeded materials could reduce side effects, toxicity, and lingering symptoms (70). Heavy metal removal, as well as other potential applications, is dependent upon the presence of a sorbent material that has the affinity and selectivity for effective toxin capture under very challenging solution conditions (i.e., high salt, high protein, low concentration of toxin, etc.) during the timeframe that the sorbent is exposed to the relevant biofluid.

This work explores the sorption efficacy and biocompatibility of SAMMS-based materials in biological matrixes. As was previously mentioned, SAMMS can be made to bind transition metals, lanthanide, or a range of radionuclides, but herein we focus upon toxic heavy metal applications. We have investigated the material performance for select heavy metals as a function of the biological matrix (blood/plasma, urine, synthetic gastrointestinal fluids, etc.) and assessed the susceptibility of these sorbent materials toward degradation and cellular uptake. General issues with the utilization of functionalized nanoporous silica for potential therapeutic and diagnostic applications are also examined.

EXPERIMENTAL SECTION

Sorbent Materials

The synthesis and characterization of the self-assembled monolayers on mesoporous silica (SAMMS) materials have been described elsewhere, including thiol (SH)-SAMMS, acetamide phosphonic acid (AcPhos)-SAMMS, glycinylurea (Gly-Ur)-SAMMS, and IDAA-SAMMS, which is based upon surface-tethered iminodiacetic acid (IDAA), which behaves analogously to the chelating ligand EDTA (1, 56, 57, 62, 76). The large-pore MCM-41 was synthesized based on the method of Sayari and co-workers (77). Specific surface areas and pore sizes were determined using an Autosorb-6B surface area analyzer (Quantachrome Corp., Boynton Beach, FL) using the Brunauer–Emmett–Teller and Barrett–Joyner–Halenda routines, with pore size values determined from the desorption data. The ligand density was determined by analysis of the organic content of the materials post-functionalization using a NETZCH STA 409 C/CD thermogravimetric analyzer. Figure 1 presents the chemical

structures of the SAMMS materials utilized in this study. Some of the basic material properties of these sorbents have been summarized in Table 1. Commercial resin values are not shown because the flexible polymer structure precludes accurate measurement of their surface area. The SH resin used in this study was GT-73, a thiol-functionalized styrene–divinylbenzene resin sorbent manufactured by Rohm and Haas Co. (Philadelphia, PA). The EDTA resin used in this study was Chelex 100, an IDAA-functionalized styrene–divinyl-benzene sorbent manufactured by Bio-Rad. The activated carbon was Darco KB-B (from Sigma-Aldrich, Milwaukee, WI).

Test Matrixes

Batch metal sorption experiments were performed in a number of different solutions. Human urine and blood were used as received, though the blood (Golden West Biologicals, Inc., Temecula, CA) contained 0.1 M sodium citrate as an anticoagulant. Rat urine was diluted 4 times prior to use. The synthetic gastric fluid (SGF) and synthetic intestinal fluid (SIF) were prepared daily following the recommendations of the U.S. Pharmacopeia for drug dissolution studies in stomach and intestine, respectively (78, 79). The SGF (pH 1.11) contained 0.03 M NaCl, 0.085 M HCl, and 0.32% (w/v) pepsin. The SIF contained 0.05 M KH_2PO_4; its pH was adjusted to 6.8 with 0.2 M NaOH. Pancreatin, a protein component, was omitted from the SIF formula because it was shown to clog filters and render analysis impractical. A modified Krebs–Henseleit buffer solution (pH 6.80) consisted of 118.0 mM NaCl, 4.7 mM KCl, 1.2 mM $MgSO_4$, 1.2 mM KH_2PO_4, 11.0 mM D-glucose, 2.5 mM $CaCl_2 \cdot 2H_2O$, and 25.0 mM $NaHCO_3$. All reagents were purchased from Sigma-Aldrich and were of the highest purity available.

Batch Metal Adsorption

Batch metal adsorption experiments were used to determine the affinity of a sorbent for a target metal species. The affinity was then quantitated via calculation of a distribution coefficient (K_d, mL/g; eq 1),

$$K_d = \frac{C_0 - C_f}{C_f} \frac{V}{M} \quad (1)$$

where C_0 and C_f are the initial and final concentrations of the target species as determined by inductively coupled plasma mass spectrometry (ICP-MS), V is the matrix volume, and M is the mass of the sorbent.

Each experiment was performed as previously described (a detailed account can be found in the Supporting Information) (80). A liquid sample was spiked using metal ion standards to obtain a known concentration of each target metal (As, Cd, Hg, and Pb). A small amount of the sorbent material suspended in deionized water was then added to the samples to obtain a desired solid-to-liquid ratio (S/L with units of g/L throughout). The sample was allowed to mix for 2 h at 160 rpm on an orbital shaker, after which it was centrifuged and the supernatant collected for analysis. The metal concentrations were determined via an Agilent 7500 inductively coupled plasma mass spectrometer after construction of calibration curves using the four metals. Each experiment was performed in triplicate.

Material Stability

Along with the K_d measurements, Si was measured via ICP-MS in the solutions before and after batch contacting with SH-SAMMS. The percent of silicon (Si) dissolved per gram of material was reported for each solution matrix as the average value of three replicates.

In Vitro Caco-2 Cell Uptake

Caco-2 cells were seeded for 21 days at 37 °C and 5% CO_2 in a transwell polycarbonate membrane culture dish (Apredica, Watertown, MA; a schematic of this apparatus is shown in the Supporting Information). SH-SAMMS was prebound with 1.0 mg of Cd, 1.0 mg of Hg, 1.0 mg of Pb, and 0.6 mg of As per gram of SH-SAMMS prior to cell exposure (see the Supporting Information). The solid was suspended in a transport buffer (pH 7.4) consisting of 1.98 g/L glucose, 10% (v/v) 10× Hank's balanced salt solution with calcium (Ca) and magnesium (Mg), and 0.01 M 4-(2-hydroxyethyl)-1-piperazineethanesulfonic acid (HEPES) buffer at a S/L ratio of 10 g/L. A 0.25 mL aliquot of this suspension was added to the apical side of the cell monolayer, and 1.0 mL of the transport buffer sans sorbent was added to the basolateral side. After 2 h, the solution from the basolateral side was collected and diluted 10-fold in 2% HNO_3 for ICP-MS analysis of the four metals (As, Cd, Hg, and Pb) and Si. Each experiment was performed in triplicate with two controls (without metal-bound SH-SAMMS).

Cell Monolayer Integrity

The integrity of the Caco-2 cell after contact with the metal-bound SH-SAMMS was assessed by measuring the transendothelial electrical resistance (TEER) of the cell monolayer after the cell uptake study mentioned above. After 2 h of incubation time, the solution in the basolateral side was replaced with 1 mL of fresh buffer and the resistance across the cell membrane was measured with the electrical cell sensor system (World Precision Instruments, Sarasota, FL). Two controls were performed using the same Caco-2 cell systems but without the addition of metal-bound SH-SAMMS.

Cell Uptake Study Using Fluorescent Dye-Tagged SH-SAMMS

SH-SAMMS was tagged with a fluorescent dye (Alexa Fluor 488, Invitrogen, Carlsbad, CA) according to our coupling procedure (see the Supporting Information). For this study, the Caco-2 cells were grown in-house (see the Supporting Information for the culture procedure), transferred to 1.5 mL of transport buffer, and exposed to fluorescent dye-tagged SAMMS at 1 $\mu g/mm^2$. After the cells and materials were allowed to incubate for 3 h, the cells were imaged while alternating between correlated differential interference contrast (DIC) and fluorescence modes on a wide-field Axiovert system from Ziess. The cells were then incubated with Trypan Blue (Sigma) for 15 min at room temperature in order to quench the fluorescence, washed with the transport buffer, and imaged again to determine the particle internalization.

RESULTS AND DISCUSSION

Comparative Sorbent Performance in Biological Matrixes

In an effort to identify an optimum sorbent material for heavy metals in biological systems, various silica-based sorbents were tested for their ability to capture As, Cd, Hg, and Pb ions in both blood- and urine-based matrices. Blood and urine are both biologically relevant test matrices that were used to establish a sorbent's therapeutic relevance and biocompatibility regarding metal capture. The different functionalized nanoporous silica sorbents selected for this work (shown in Figure 1 and Table 1) are known to be effective at binding heavy metals, although the different surface chemistries result in different binding mechanisms, which impacts the affinity and selectivity. The absolute and relative affinity of each sorbent is based on a number factors including the porosity of the silica support, surface area, ligand density, and interaction of the material with the sample matrix. The smaller size of the thiolpropyl ligand (Figure 1) enables higher surface ligand densities (Table 1), which likely contribute to its superior performance (shown subsequently). The ability of these materials to bind and remove heavy metal ions in both blood and urine is presented in Tables 2 and 3,

respectively. The affinity of the sorbent for a target species is represented in terms of a distribution coefficient, K_d (mL/g), which is a mass-normalized partition coefficient between the solid sorbent phase and the liquid solution phase. K_d is an experimental value obtained through metal concentration measurements before and after metal sorption has occurred. Typically, the higher the K_d values, the better the sorbent. It should be pointed out that proteins are known to complex metal ions; thus, a large portion of the heavy metals in biological solutions will not be free ions but rather some other species. Furthermore, metal ions are known to interact with the various forms of inorganic (e.g., carbonates and phosphates) anions present in the biological fluids. Consequently, the metal speciation can be very complex and will depend strongly upon the specific analtye and solution conditions. High efficacy sorbents must be able to outcompete the other reactive species in solution for the available metal ions.

The values presented in Table 2 highlight thiol-based SAMMS as the superior sorbent with regards to heavy-metal capture from blood. Although overall the K_d values remain generally low because of the complex nature of the matrix, SH-SAMMS binds each metal approximately 2 orders of magnitude better than most of the other sorbents (most notably the commercial thiol resin and activated carbon). The urine sorption data in Table 3 are less decisive, but a similar trend is observed with SH-SAMMS, representing the best general sorbent for the metals tested. These results are somewhat expected because the softer thiol ligands would be predicted to bind the softer heavy metals better than the harder, more oxygenated ligands installed on the other SAMMS materials studied. The thiol resin, on the other hand, bound metals in the urine matrix with a lower affinity than both the SH-SAMMS and other commercial materials and proved incapable of binding metals in blood. This is an interesting result because one might expect closely related binding and similar trends to be observed between the resin and functionalized silica because of their similar surface chemistries. This divergent binding may be due to a number of factors but is principally due to the higher surface area coupled with the highly ordered monolayer interface of the SAMMS sorbent, allowing multiple metal–ligand interactions, as well as the greater tendency of the polymeric resin to accumulate protein fouling. The high-density monolayer allows metal cations to interact with multiple thiol groups, resulting in stronger binding interactions as opposed to the randomly ordered copolymer resin, in which the metal cations are most likely interacting with a single thiol group.

EDTA has been recognized as a powerful complexant and has a range of biological applications. Both commercial and SAMMS-based EDTA-like sorbents proved capable of capturing metals from the biological solution and showed similar complexation trends. EDTA is a relatively hard ligand system composed of carboxylic acids and amines. As a result, these sorbents were better at capturing the harder transition metals like Cd and Pb than the softer metals like As and Hg. AcPhos- and Gly-Ur-SAMMS were designed specifically to bind rare-earth cations and, not surprisingly, showed little to no binding for Cd, Hg, or Pb in either solution, thus demonstrating that these ligand systems have too low of an affinity to be effective sorbents for “soft” heavy meals in biological matrixes (although they may be good ligands for the selective capture of rare-earth cations in biological matrixes).

With its high surface area, ligand density, and affinity, SH-SAMMS generally outperformed the commercial sorbents for the softer heavy metals. Activated carbon has a high surface area but possesses harder ligands (e.g., carboxylates, phenols, etc.), which are less ordered, resulting in a more random coordination with the metal ions and thus a lower-affinity surface chemistry. Activated carbon was only effective at capturing Pb from the blood matrix but was capable of binding Cd, Hg, and Pb in urine. Only for the capture of Pb in urine was activated carbon an improvement over SH-SAMMS.

The K_d values in Tables 2 and 3 show that thiol-functionalized mesoporous silica will serve as an effective heavy-metal sorbent in biological systems. The data from Table 2 show SH-SAMMS to be a vastly preferred sorbent material for any blood-based applications. To be effective as an orally delivered treatment, the material must meet the following criteria: it must have high affinity for the target metals among the nontarget metals in an assortment of relevant matrices (e.g., blood, urine, low-pH gastric fluid, near-neutral-pH intestinal fluid, etc.), sufficiently rapid metal binding rates, large sorption capacity (e.g., not saturated with the nontarget metals), long-term stability so as not to facilitate the release of captured metal ions, and the ability to function in high concentrations of biomolecules and resist the nonspecific adsorption of proteins, and it must resist cellular uptake while not damaging the cell. These criteria are investigated for therapeutic and diagnostic applications in subsequent sections.

Sorbent Affinity as a Function of the Sample Matrix

SH-SAMMS metal uptake was examined in a variety of sample matrices. Matrices were chosen not only with regard to their biological relevance but also to help gain an understanding of metal uptake as a function of the protein content, pH, and ionic strength. Biologically relevant solutions included dilute rat urine, normal human urine, whole human blood, and synthetic gastric and intestinal fluids (SGF and SIF, respectively). Both synthetic gastric and intestinal fluids used in this work were prepared according to the formula recommended by the U.S. Pharmacopeia for drug dissolution study in mammals (78, 79). Table 4 compares the K_d values obtained for the four metals and SH-SAMMS measured in these solutions.

Previous work has shown that thiol-SAMMS has a high affinity for Hg, Cd, and Pb in natural waters, with K_d values in excess of 10^4 and occasionally exceeding 10^6 (81). Inspection of the data in Table 4 shows that K_d values are smaller in biological matrices than in natural waters. SH-SAMMS shows a decrease in the metal uptake for experiments performed in urine and blood compared to natural waters. One possible explanation for the reduction in the K_d values in natural water versus biological matrices is with regard to the available protein content. As the relative protein concentration of the sample matrix is increased (dilute urine < concentrated whole urine < blood), the K_d values are generally observed to decrease.

The term “biofouling” is often used to describe a drop in the performance or efficiency of a material due to the presence of a large quantity of biomolecules. The increased presence of protein is capable of negatively impacting the sorbent performance in a number of ways. Physisorption of the biomolecules to either the interior or exterior surface of the mesoporous silica could result in significantly decreased ligand–metal interaction. Protein interaction with the available thiol ligands is also conceivable because of the large degree of disulfide linkages and other potentially reactive sites present throughout protein structures. Prevention or reduction of biofouling caused by any (or all) of these mechanisms would lead to improved sorbent performance in biological fluids, thus expanding their applicability.

Also of note is the increased performance of the large-pore SH-SAMMS relative to the smaller-pore samples in the blood matrix. This result makes sense if taken in the context of potential pore blockage. The data indicate the greater uptake ability of the large-pore SAMMS possibly due to the decreased pore blockage that arises simply from having larger pores. Decreased pore blockage allows greater access of the metal ion to the bulk of the silica surface area inside the pores, resulting in increased ligand–metal binding. These results indicate the need for a more extensive study of metal uptake with regard to the sorbent pore size. Despite this increased uptake, however, the large-pore SAMMS still experiences a large degree of protein fouling, as evidenced by the considerable loss in

uptake ability relative to experiments performed in “protein-free” matrices (Supporting Information). In order to eventually realize the optimal potential of these materials for heavy metal detection and detoxification therapeutics, efforts must be made to reduce biofouling.

Sorbent Affinity as a Function of the pH

Any potential oral therapeutic is going to be subjected to a range of solution conditions on its journey through the body. Insight into how a material behaves and is impacted by each of these changing conditions is vital toward achieving a complete understanding of the material’s therapeutic potential. The solution pH is one of these conditions, ranging from highly acidic to slightly basic (pH ~1–8.5), depending on the region of the body. For example, the pH range of the biological matrices discussed in this report range from pH 1.1 in SGF to pH 7.5 in blood (Table 4) and is known to be as high as 8.3 in various regions of the gastrointestinal tract.

The K_d values of As, Cd, Hg, and Pb on SH-SAMMS as a function of the solution pH are reported in Figure 2. The solutions were prepared by adjusting the pH of the SGF (an initial pH of 1.11) with 0.2 M $NaHCO_3$ in order to achieve a pH similar to what might be encountered within the different regions of the gastrointestinal tract (pH 1–3 in stomach, pH 5.5–7 in large intestine, pH 6–6.5 in duodenum, and pH 7–8 in jejunum and ileum) (82). It should be noted that the SH-SAMMS affinity for all analytes remains stable or increases with rising pH, which correlates to the pH trend in the gastrointestinal tract, suggesting that captured metals will not be leached out by the changing intestinal environments.

The high binding affinity (K_d ~ 106) observed for Hg across the entire pH range is expected and has previously been reported for SH-SAMMS in acidic wastewater (1). This binding consistency indicates that the thiol surface remains active throughout the pH range encountered in the gastrointestinal tract. While speciation in the biological solution can be complex, the observed pH-dependent adsorption of Cd and Pb ions can likely be attributed to the hydrolysis behavior of these ions over the pH range because a similar behavior has been observed in aquatic matrices (83–85). The K_d value of As was high at pH 1.1 (K_d ~ 17 000), decreased to by a factor of 10 as the pH increased from 1.1 to 4.0, and rose again as the pH became more neutral (5.6–8.3). As the pH increases, the emergence of negatively charged species (i.e., $H_2AsO_4^-$ and $HAsO_4^{2-}$) becomes more prevalent, with the divalent nature of the latter species allowing for interaction with multiple thiol ligands, thus resulting in a significant increase in the overall affinity, as observed with Cd and Pb. The increase in K_d at lower pH for As is not completely understood, but the data do suggest a high affinity between completely protonated thiols and neutral arsenic species, H_3AsO_4 and H_3AsO_3, which are the dominant species under acid conditions (86).

Sorbent Affinity as a Function of the Ionic Strength

Several oral drugs rely on ion-exchange resins for capturing undesirable toxins, such as sodium poly(styrenesulfonate), a cation-exchange resin for capturing excess potassium, and cross-linked allylamine hydrochloride, an anion-exchange resin for binding with phosphate in the gastrointestinal tract (87). Unfortunately, however, polymer resins have been known to suffer from swelling and shrinking caused by a variation in the solution ionic strength, threatening to retard the therapeutic properties of these resin-based drugs. The ionic strengths experienced by a sorbent in biological matrices tend to be greater than that of most natural waters (seawater being the primary exception). Conductivity measurements, in general, show a 10-fold increase in the ionic strength in biological matrixes, such as blood and urine, compared to river water and ground-water (Table 4 and Supporting Information). In order to evaluate the performance of SH-SAMMS as a function of the ionic strength, heavy metal uptake was measured throughout a range of ionic strengths, achieved by

varying the concentration of a sodium acetate buffer matrix. The data for SH-SAMMS indicate that increasing the concentration of the sodium acetate buffer from 0.001 to 0.1 M has very little effect on the affinity of the sorbent for the four metals (Supporting Information), consistent with similar results in ionic solutions (56). Only when the acetate concentration was increased to 1 M did the affinity for Pb and Cd decrease by about 10-fold, while still retaining a relatively high K_d (>105). The K_d values for both Hg and As remained uniformly high throughout the range of ionic strengths. Consequently, variations in the biologically relevant ionic strengths are unlikely to significantly impact chelation of these four metals by SH-SAMMS.

Adsorption Kinetics and Capacity

Fast sorption kinetics are typically therapeutically and diagnostically beneficial. For some applications of oral drugs, fast kinetics could be particularly valuable because it limits the amount of time that toxins would be bioavailable, thereby limiting the amount absorbed into the human body. Detailed sorption kinetics of Hg in SGF and of Cd in SIF are available in the Supporting Information. Over 99% of Hg in SGF and Cd in SIF were removed after 3 min. This rapid sorption rate is due to the rigid pore structure and mesoporous size, which allows constant exposure to a greater number of available thiol binding sites, in contrast to the swellable polymer ion-exchange resins such as GT-73 (54). From 2 to 24 h of contact time, the extent of sorption remains steady, indicating that there is no significant leaching of Hg and Cd from the laden sorbent and no significant degradation of the materials in these two matrices.

Adsorption capacity data were obtained for Hg in SGF, Cd in SIF, and As in both SGF and SIF (Supporting Information). The matrices were chosen on the basis of their affinities for binding SH-SAMMS exhibited in Table 4. The adsorption data for each metal are very consistent with a Langmuir adsorption model ($R^2 > 0.99$), strongly suggesting monolayer adsorption without precipitation of the metal ions out of the solutions at these conditions. The maximum sorption capacities for Hg, Cd, and As, as estimated by Langmuir isotherm models are summarized in Table 5. While the measured capacities in Table 5 are lower than some reported in the literature, the uptake capacities are still very good because of the high affinity of SH-SAMMS for the target metals. The reduction of capacities is likely due, in part, to the presence of high concentrations of other ions in the test solutions (NaCl, KCl, and KH_2PO_4) when compared to less complex matrices such as distilled water or ground-water. Furthermore, the acidity of the SGF increases the protic competition for the binding sites (compared to near-neutral solutions), resulting in a lower overall capacity (1, 88). A similar trend has been observed in less complex matrices such as acidified water (1).

The adsorption isotherm of Pb in SIF could not be measured in the same fashion with others because of the high degree of Pb precipitation in the high-phosphate matrix. However, on the basis of the affinity data in Table 4, Pb is predicted to have an absorption capacity between those of the other metals. Table 5 also indicates that an increase in the temperature from room temperature (24 °C) to body temperature (37 °C) has little effect on As sorption on SH-SAMMS, which is generally expected for covalent bonding or monolayer chemical adsorption. Thus, most batch sorption experiments in this work were measured at room temperature.

Material Stability

Whereas material stability might not be very important for short-term sorbent applications (e.g., such as contaminant detection or analysis), longer term and in vivo human applications, such as the majority of those discussed herein, would seek to limit material degradation. For this reason, the extent of SAMMS stability was determined by monitoring

dissolved Si after the solution had been exposed to the SAMMS sorbent. The weight percents of Si dissolved per total mass of SH-SAMMS after 2 h of stirring in acidic (pH 1.1) and near-neutral (pH 6.8) fluids were measured. Very little leaching was observed, 0.2% (pH 1.1) and 2% (pH 6.8) Si loss by weight, showing good material stability for the tested conditions. Because of the strong covalent bonding between the monolayers and the substrate as well as the high degree of cross-linking among the thiol monolayers, the Si dissolved is suspected to come from the residual (and physisorbed) poly(mercaptopropylsiloxane) used in the SH-SAMMS synthesis rather than the monolayer degradation (the latter would result in a decrease in the binding capacity). The materials also possess a good shelf-life, having demonstrated the same metal binding performance after 5 years of storage, with longer effective material lifetimes probable (67).

Cell Uptake and Cell Integrity

In order to serve as a potential detoxification therapeutic, the sorbent materials must not only maintain a high affinity for the target metals but also remain relatively inert with regard to the types of cells and biomolecules encountered in the body. An ideal material would minimize cellular interaction in a manner that avoids damage to the cell while preventing release of the captured metals. Consequently, cellular uptake studies were performed to assess the level of interaction between cells and SAMMS material in vitro. Caco-2 cells were utilized for these studies because they possess many of the properties of the small intestinal epithelium and have been used previously to determine transport of chemicals across the human intestinal epithelium (89–91).

Prior to incubation with cells, the ability of the SH-SAMMS material to maintain metal chelation was assessed. The SH-SAMMS material that had been prebound with 1.0 mg/g sorbent each of Cd, Pb, and Hg and 0.6 mg/g of As was suspended in solution for 30 min. No detectable leaching of Cd, Pb, and Hg and only a small leachate of Si and As (0.1 and 0.3 wt %, respectively) were observed via ICP-MS during this period of time, indicating the ability of the SAMMS material to retain bound metals. For cellular uptake studies, Caco-2 cells were cultured for 21 days in a transwell poly-carbonate membrane culture dish before use to investigate the transport of SAMMS across the epithelial cells. Cell membrane permeability is evaluated through the cell's ability to grow into a monolayer atop a permeable filter support. Material is added to either the apical or basolateral side of the monolayer and allowed to incubate. Mass spectrometry analysis of the solution from both sides then gives valuable insight into the permeability of the drug or material. This type of assay is often used to make in vivo predictions as to the bioavailability of a potential drug based on in vitro experiments.

For this study, the preloaded SAMMS material was suspended in a transport buffer, added to the apical side of the monolayer, and allowed to incubate for 2 h. Samples for detection were then taken from the basolateral side. The metal concentrations detected in these samples are listed in Table 6 and represent a measure of the ability of the material to permeate and transport across the cell monolayer. The data indicate no difference in the concentrations of the four metals on the basolateral side between the test and control groups (with no metal-bound SAMMS material added), signifying a lack of cell permeability. This ability to resist cellular uptake is likely due to the relatively large particle size of SH-SAMMS (95% of the material is larger than 5 μm, and the mean particle size is 22 μm, compared to a cell diameter of approximately 10 μm) because previous studies have indicated that materials with much smaller dimensions (~50 nm in diameter) tend to be susceptible to uptake. TEER measurements (Table 6) were taken to gauge the integrity of the monolayer postincubation with the SAMMS material. No difference between cells that were exposed to the materials and the control cells was observed, suggesting that the metal-bound SAMMS are not damaging the cells.

A series of DIC and fluorescence images, taken through the *z*-axis of the cells after exposure to fluorescent dye-tagged SH-SAMMS, confirm this lack of uptake. The fluorescently tagged material was incubated with the cells for 3 h, followed by fluorescence quenching by Trypan Blue (Figure 3). Although larger particles (>5 μm) can be observed to be stuck to the cell surface, none of these particles seem to permeate the cell membrane. Only the smallest particles (<1 μm) appear to enter the cell cytoplasm. Also of note, no change in the morphology of the cells was observed in the presence of the larger particles, when compared with control cells (not shown).

Chelating of Essential Minerals

One of the drawbacks of EDTA chelation that is commonly employed for detoxification therapy is that it facilitates urinary excretion of essential minerals, especially Ca (by 2-fold) and Zn (by 18-fold) (50). Consequently, the uptake of essential minerals by SH-SAMMS was examined using similar concentrations encountered in vivo. We found that SH-SAMMS did not significantly remove 100 mg/L of Ca, 30 mg/L of Mg, 0.5 mg/L of Fe^{III}, and 0.5 mg/L of Mo in both the low-pH SGF and near-neutral pH SIF (an alternative form of SIF, modified Kreb's buffer, was used in this study to better solubilize the minerals of interest). This observation is in line with the hard–soft acid–base (HSAB) theory that predicts the soft thiol ligand would have a very low affinity for hard metals such as Ca, Mg, and Fe (92). A total of 0.5 mg/L of Zn and Cu was also investigated; however, the metals could largely be collected by 0.45 μm filters (even in the absence of sorbent), making it difficult to assess their uptake on SH-SAMMS. Thus, Zn and Cu excretion facilitated by SH-SAMMS will be measured in a future in vivo study. However, we predict that both Zn and Cu, which are borderline metals according to the HSAB principle, would likely be captured by SH-SAMMS but to a much lower degree than "soft" heavy metals (like Hg). Previous results showing SH-SAMMS to have a much lower affinity for Zn than for Hg support this prediction (1).

CONCLUSIONS

A number of commercial and mesoporous silica-based sorbent materials with various surface chemistries were analyzed in vitro to assess their viability as oral therapeutics for the removal of internalized heavy metals. In general, SH-SAMMS proved to be the most effective sorbent materials for heavy-metal sorption from biological matrices such as blood, urine, and synthetic gastric and intestinal fluids. The performance of the thiol-functionalized material remained relatively unperturbed throughout relevant pH and ionic strength ranges and was shown to only minimally degrade over an extended period of time in both neutral and acidic pH values. Additionally, cellular uptake studies demonstrated no cell membrane permeation by the silica-based materials, generally highlighting the materials cellular biocompatibility. Finally we found that SH-SAMMS did not remove essential elements such as Ca, Mg, and Fe from bodily fluids, thus offering an improvement over the more traditional EDTA chelation methods whose nondiscriminatory metal-binding properties have been known to cause death. Taken in concert, these results suggest that improvements in heavy metal chelation and detoxification therapies may be achieved through high-performance orally administered high-efficacy sorbents, such as those demonstrated with SH-SAMMS for the softer heavy metals. A preclinical evaluation to assess the in vivo efficacy of the SH-SAMMS material for heavy metal removal would be needed to further gauge the efficacy of these materials. Additionally, we acknowledge that while the SH-SAMMS sorbent did prove the most capable material for removing the majority of the available heavy metals in biological solutions, there remains an opportunity for additional performance improvement. Further investigations aimed at understanding and minimizing the deleterious interactions (e.g., protein interference) in biological fluids as well as improving material efficacy through

improved surface chemistry and material structure are currently underway. Different surface chemistries are also being explored for other theranostic applications. This focused heavy metal detoxification study is an initial proof of concept demonstration. The design and development of advanced sorbent materials with high efficacy in biological fluids should enable a broad range of beneficial therapeutic methods and diagnostic tools.

Supplementary Material

Refer to Web version on PubMed Central for supplementary material.

Acknowledgments

The work was supported by the National Institute of Environmental Health Sciences (grant R21 ES015620) and the National Institute of Allergy and Infectious Disease (Grants R01-AI074064 and R01-AI080502). The research was performed, in part, at the Environmental Molecular Sciences Laboratory, a DOE national scientific user facility located at PNNL. The authors thank View Koonsiripaiboon, Jarupa Kanlayanatham, Joseph D. Davidson, Dr. George A Porter, Dr. Worapon Kiatkittipong, Dr. Joongjai Panpranot, and Dr. Karla Thrall for their contributions.

REFERENCES AND NOTES

1. Feng X, Fryxell GE, Wang LQ, Kim AY, Liu J, Kemmer KM. Science. 1997; 276:923–926.
2. Delacote C, Gaslain FOM, Lebeau B, Walcarius A. Talanta. 2009; 79:877–889. [PubMed: 19576459]
3. Lei C, Shin Y, Magnuson JK, Fryxell GE, Lasure LL, Elliott DC, Liu J, Ackerman EJ. Nanotechnology. 2006; 17:5531–5538. [PubMed: 21727320]
4. Chen B, Lei C, Shin Y, Liu J. Biochem Biophys Res Commun. 2009; 390:1177–1181. [PubMed: 19874798]
5. Avnir D, Coradin T, Lev O, Livage J. J Mater Chem. 2006; 16:1013–1030.
6. Lei C, Soares TA, Shin Y, Liu J, Ackerman EJ. Nanotechnology. 2008; 19:125102. [PubMed: 21817721]
7. Lei C, Shin Y, Liu J, Ackerman EJ. Nano Lett. 2007; 7:1050–1053. [PubMed: 17341123]
8. Bellino MG, Regazzoni AE, Soler-Illia GJAA. ACS Appl Mater Interfaces. 2010; 2:360–365. [PubMed: 20356181]
9. Klichko Y, Liong M, Choi E, Angelos S, Nel AE, Stoddart JF, Tamanoi F, Zink JI. J Am Ceram Soc. 2009; 92:S2–S10. [PubMed: 19834571]
10. Lin YS, Tsai CP, Huang HY, Kuo CT, Hung Y, Huang DM, Chen YC, Mou CY. Chem Mater. 2005; 17:4570–4573.
11. Torney F, Trewyn BG, Lin VSY, Wang K. Nat Nanotechnol. 2007; 2:295–300. [PubMed: 18654287]
12. Tan W, Wang K, He X, Zhao XJ, Drake T, Wang L, Bagwe RP. Med Res Rev. 2004; 24:621–638. [PubMed: 15224383]
13. Ostafin AE, Siegel M, Wang Q, Mizukami H. Microporous Mesoporous Mater. 2003; 57:47–55.
14. Gianotti E, Bertolino CA, Benzi C, Nicotra G, Caputo G, Castino R, Isidoro C, Coluccia S. ACS Appl Mater Interfaces. 2009; 1:678–687. [PubMed: 20355990]
15. Innocenzi P, Lebeau B. J Mater Chem. 2005; 15:3821–3831.
16. Ow H, Larson DR, Srivastava M, Baird BA, Webb WW, Wiesner U. Nano Lett. 2005; 5:113–117. [PubMed: 15792423]
17. Tsai CP, Hung Y, Chou YH, Huang DM, Hsiao JK, Chang C, Chen YC, Mou CY. Small. 2008; 4:186–191. [PubMed: 18205156]
18. Lu J, Liong M, Sherman S, Xia T, Kovochich M, Nel AE, Zink JI, Tamanoi F. NanoBiotechnology. 2007; 3:89–95. [PubMed: 19936038]
19. Burns A, Ow H, Weisner U. Chem Soc Rev. 2006; 35:1028–1042. [PubMed: 17057833]
20. Fuller JE, Zugates GT, Ferreira LS, Ow HS, Nguyen NN, Wiesner UB, Langer RS. Biomaterials. 2008; 29:1526–1532. [PubMed: 18096220]

21. Tang QL, Xu Y, Wu D, Sun YH, Wang J, Xu J, Deng F. J Controlled Release. 2006; 114:41–46.
22. Charnay C, Begu S, Tourne-Peteilh C, Nicole L, Lerner DA, Devoisselle JM. Eur J Pharm Biopharm. 2004; 57:533–540. [PubMed: 15093603]
23. Vallet-Regi M, Ramila A, del Real RP, Perez-Pariente J. Chem Mater. 2001; 13:308–311.
24. Munoz B, Ramila A, Diaz I, Perez-Pariente J, Vallet-Regi M. Chem Mater. 2003; 15:500–503.
25. Ramila A, Munoz B, Perez-Pariente J, Vallet-Regi MJ. Sol–Gel Sci Technol. 2003; 26:1199–1202.
26. Doadrio AL, Sousa EMB, Doadrio JC, Perez-Pariente J, Izquierdo-Barba I, Vallet-Regi M. J Controlled Release. 2004; 97:125–132.
27. Vallet-Regi M, Doadrio JC, Doadrio AL, Izquierdo-Barba I, Perez-Pariente J. Solid State Ionics. 2004; 172:435–439.
28. Horcajada P, Ramila A, Perez-Pariente J, Vallet-Regi M. Microporous Mesoporous Mater. 2004; 68:105–109.
29. Trewyn BG, Whitman CM, Lin VSY. Nano Lett. 2004; 4:2139–2143.
30. Lai CY, Trewyn BG, Jeftinifa DM, Jeftinifa K, Xu S, Jeftinifa S, Lin V. J Am Chem Soc. 2003; 125:4451–4459. [PubMed: 12683815]
31. Zeng W, Qian XF, Zhang YB, Yin J, Zhu ZK. Mater Res Bull. 2005; 40:766–772.
32. Vallet-Regi M, Ruiz-Gonzalez L, Izquierdo-Barba I, Gonzalez-Calbet JM. J Mater Chem. 2006; 16:26–31.
33. Zeng W, Qian XF, Yin J, Zhu ZK. Mater Chem Phys. 2006; 97:437–441.
34. Perez-Quintanilla D, Gomez-Ruiz S, Zizak Z, Sierra I, Prashar S, Hierro Id, Fajardo M, Juranic ZD, Kaluderovic GN. Chem— Eur J. 2009; 15:5588–5597. [PubMed: 19370742]
35. Lu J, Liong M, Zink JI, Tamanoi F. Small. 2007; 3:1341–1346. [PubMed: 17566138]
36. DiPasqua AJ, Sharma KK, Shi YL, Toms BB, Ouellette W, Dabrowiak JC, Asefa T. J Inorg Biochem. 2008; 102:1416–1423. [PubMed: 18279965]
37. Lu J, Choi E, Tamanoi F, Zink JI. Small. 2008; 4:421–426. [PubMed: 18383576]
38. ATSDR. Toxicological profile for cadimum. Department of Health and Human Services; WAshingotn, DC: Jul. 1999
39. UNEP DTIE Chemicals Branch and WHO Department of Food Safety, Z., and Foodborne Disease. Guidance for identifying populations at risk for mercury exposures. Geneva, Switzerland: Aug. 2008
40. Satarug S, Garrett SH, Sens MA, Sens DA. Environ Health Perspect. 2009; 118(2):XXX.
41. Wiggers GA, Pecanha FM, Briones AM, Perez-Giron JV, Miguel M, Vassallo D, Cachofeiro V, Alonso MJ, Salaices M. Am J Physiol Heart Circ Physiol. 2008; 295:H1033–H1043. [PubMed: 18599595]
42. Toscano CD, Guilarte TR. Brain Res Rev. 2005; 49(3):529–554. [PubMed: 16269318]
43. Counter SA, Buchanan LH. Toxicol Appl Pharmacol. 2004; 198(2):209–230. [PubMed: 15236954]
44. Vahter M. Annu Rev Nutr. 2009; 29(1):381–399. [PubMed: 19575603]
45. Díez, S. Reviews of Environmental Contamination and Toxicology. Vol. 198. Springer; New York: 2009. Human health effects of methylmercury exposure; p. 1-22.
46. Wild P, Bourgkard E, Paris C. Cancer Epidemiol. 2009:139–167.
47. Barbier O, Jacquillet G, Tauc M, Cougnon M, Poujeol P. Nephron Physiol. 2005; 99(4):105–110.
48. Yantasee W, Charnhattakorn B, Fryxell GE, Timchalk C, Addleman RS. Anal Chim Acta. 2008; 620:55–63. [PubMed: 18558124]
49. Yantasee W, Lin Y, Hongskirikam K, Fryxell GE, Addleman R, Timchalk C. Environ Health Perspect. 2007; 115:1683–1690. [PubMed: 18087583]
50. Waters R, Bryden N, Patterson K, Veillon C, Anderson R. Biol Trace Element Res. 2001; 83:207–221.
51. Brown MJ, Willis T, Omalu B, Leiker R. Pediatrics. 2006; 118:e534–e536. [PubMed: 16882789]
52. FDA approves first new drug application for the treatment of radiation contamination due to cesium or thallium. http://www.fda.gov/Drugs/EmergencyPreparedness/BioterrorismandDrugPreparedness/ucm130335.htm

53. Fryxell, GE.; Addleman, RS.; Mattigod, SV.; Lin, Y.; Zemanian, TS.; Wu, H.; Birnbaum, JC.; Liu, J.; Feng, X. Environmental and sensing applications of molecular self-assembly. In: Schwarz, JA.; Contescu, C.; Putyera, K., editors. Dekker Encyclopedia of Nanoscience and Nanotechnology. Marcel Dekker; New York: 2004. p. 1135-1145.
54. Yantasee W, Warner CL, Addleman RS, Carter TG, Wiacek RJ, Fryxell GE, Timchalk C, Warner MG. Environ Sci Technol. 2007; 41:5114–5119. [PubMed: 17711232]
55. Johnson BE, Santschi PH, Addleman RS, Douglas M, Davidson JD, Fryxell GE, Schwantes JM. Appl Radiat Isot. 201010.1016/j.apradiso.2010.07.025
56. Chen X, Feng X, Liu J, Fryxell GE, Gong M. Sep Sci Technol. 1999; 34:1121–1132.
57. Yantasee W, Lin Y, Fryxell GE, Busche BJ, Birnbaum J. Sep Sci Technol. 2003; 38:3809–3825.
58. Walcarius A, Mercier L. J Mater Chem. 2010; 20:4478–4511.
59. Sangvanich T, Sukwarotwat V, Wiacek RJ, Grudzien RM, Fryxell GE, Addleman RS, Timchalk C, Yantasee W. J Hazard Mater. 2010; 182:225–231. [PubMed: 20594644]
60. Yantasee W, Sangvanich T, Creim JA, Pattamakomsan K, Wiacek RJ, Fryxell GE, Addleman RS, Timchalk C. Health Phys. 2010; 2010:413–419. [PubMed: 20699706]
61. Timchalk C, Creim JA, Sukwarotwat V, Wiacek R, Addleman RS, Fryxell GE, Yantasee W. Health Phys. 2010; 99:420–429. [PubMed: 20699707]
62. Busche BJ, Wiacek RJ, Davison JD, Koonsiripaiboon V, Yantasee W, Addleman RS, Fryxell GE. Inorg Chem Commun. 2009; 12:312–315. [PubMed: 22068901]
63. Fryxell GE, Mattigod SV, Lin Y, Wu H, Fiskum SK, Parker KE, Zheng F, Yantasee W, Zemanian TS, Addleman RS, Liu J, Xu J, Kemner KM, Kelly S, Feng X. J Mater Chem. 2007; 17:2863–2874.
64. Yoshitake H, Yokoi T, Tatsumi T. Chem Mater. 2003; 15:1713–1721.
65. Yokoi T, Tatsumi T, Yoshitake H. J Colloid Interface Sci. 2004; 274:451–457. [PubMed: 15144816]
66. Fryxell GE, Liu J, Gong M, Hauser TA, Nie Z, Hallen RT, Qian M, Farris KF. Chem Mater. 1999; 11:2148–2154.
67. Yantasee W, Fryxell GE, Porter GA, Pattamakomsan K, Sukwarotwat V, Chouyyok W, Koonsiripaiboon V, Xu J, Raymond KN. Nanomed Nanotechnol Biol Med. 2010; 6:1–8.
68. Grobner T. Nephrol, Dial, Transplant. 2006; 21:1104–1108. [PubMed: 16431890]
69. Borchardt PE, Yuan RR, Miederer M, McDevitt MR, Schienberg DA. Cancer Res. 2003; 63:5084–5090. [PubMed: 12941838]
70. Lewington VJ. Phys Med Biol. 1996; 41(10):2027. [PubMed: 8912378]
71. Pagel JM, Boerman OC, Breitz HB, Meredith RF. Princ Cancer Biother. 2009:463–496.
72. Holland JP, Williamson MJ, Lewis JS. Mol Imaging. 2010; 9(1):1–20. [PubMed: 20128994]
73. Desoize B, Madoulet C. Crit Rev Oncol/Hematol. 2002; 42:317–325.
74. McWhinney SR, Goldberg RM, McLeod HL. Mol Cancer Ther. 2009; 8(1):10–16. [PubMed: 19139108]
75. Kaushal GP, Kaushal V, Herzog C, Yang C. Autophagy. 2008; 4(5):710–712. [PubMed: 18497570]
76. Fryxell GE, Lin Y, Fiskum S, Birnbaum JC, Wu H, Kemmer K, Kelly S. Environ Sci Technol. 2005; 39:1324–1331. [PubMed: 15787373]
77. Sayari A, Yang Y, Kruk M, Jaroniec M. J Phys Chem B. 1999; 103:3651–3658.
78. United States Pharmacopeial Convention Inc. Rockville, MD: 1990.
79. United States Pharmacopeial Convention Inc. Rockville, MD: 2003.
80. Yantasee W, Fryxell GE, Addleman RS, Wiacek RJ, Koonsiripaiboon V, Pattamakomsan K, Sukwarotwat V, Xu J, Raymond KN. J Hazard Mater. 2009; 168:1233–1238. [PubMed: 19345006]
81. Samuels WD, LaFemina NH, Sukwarotwat V, Yantasee W, Li XS, Fryxell GE. Sep Sci Technol. 2010; 45:228–235. [PubMed: 23390326]
82. Shargel, L.; Yu, ABC. Biopharmaceutics. In: Swarbrick, J.; Boylan, JC., editors. Encyclopedia of pharmaceutical technology. 2. Vol. 1. Marcel Dekker, Inc; New York: 2002. p. 156-176.

83. Richens, DT. The Chemistry of Aqua Ions. John Wiley & Sons Ltd; West Sussex, U.K: 1997.
84. Helm L, Merbach AE. Coord Chem Rev. 1999; 187:151–181.
85. Fontenot, SA.; Carter, TG.; Johnson, DW.; Addleman, RS.; Warner, MG.; Yantasee, W.; Warner, CL.; Fryxell, GE.; Bays, JT. Nanostructured Materials for Selective Collection of Trace-Level Metals from Aqueous Systems. In: Pierce, DT.; Zhao, JX., editors. Trace Analysis with Nanomaterials. Wiley-VCH Verlag GmbH & Co; Weinheim, Germany: 2010.
86. Wang S, Mulligan CN. Sci Total Environ. 2006; 366:701–721. [PubMed: 16203025]
87. Amiji, MM. Applied Physical Pharmacy. McGraw-Hill Professional; New York: 2002.
88. Chen X, Feng X, Liu J, Fryxell GE, Gong M. Sep Sci Technol. 1999; 34:1121–1132.
89. Bhardwaj RK, Glaeser H, Becquemont L, Klotz U, Gupta SK, Fromm MF. J Pharmacol Exp Ther. 2002; 302:645–650. [PubMed: 12130727]
90. Luo FR, Paranjpe PV, Guo A, Rubin E, Sinko P. Drug Metab Dispos. 2002; 30:763–770. [PubMed: 12065434]
91. Wantanabe K, Sawano T, Terada K, Endo T, Sakata M, Sato J. Biol Pharm Bull. 2002; 25:885–890. [PubMed: 12132663]
92. Pearson RG. J Am Chem Soc. 1963; 85:3533–3539.

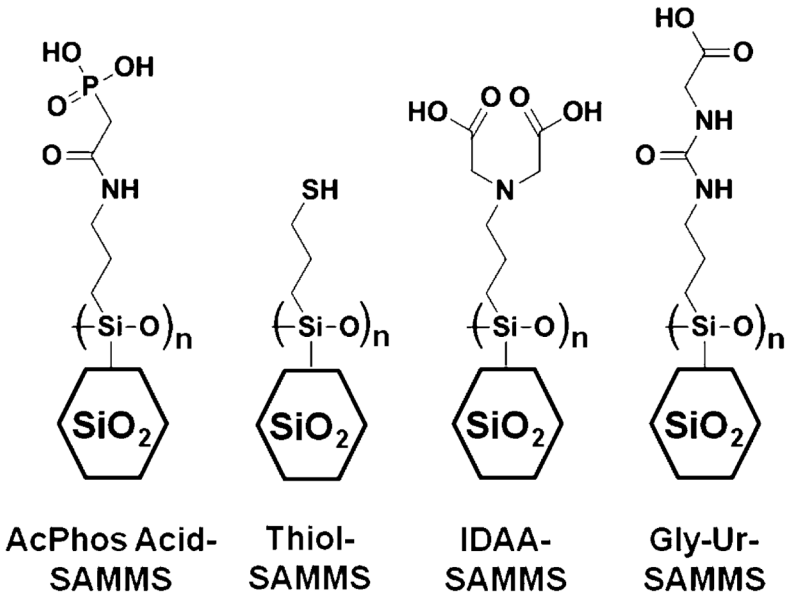

FIGURE 1.
Schematic of the organic ligand monolayers utilized in this study.

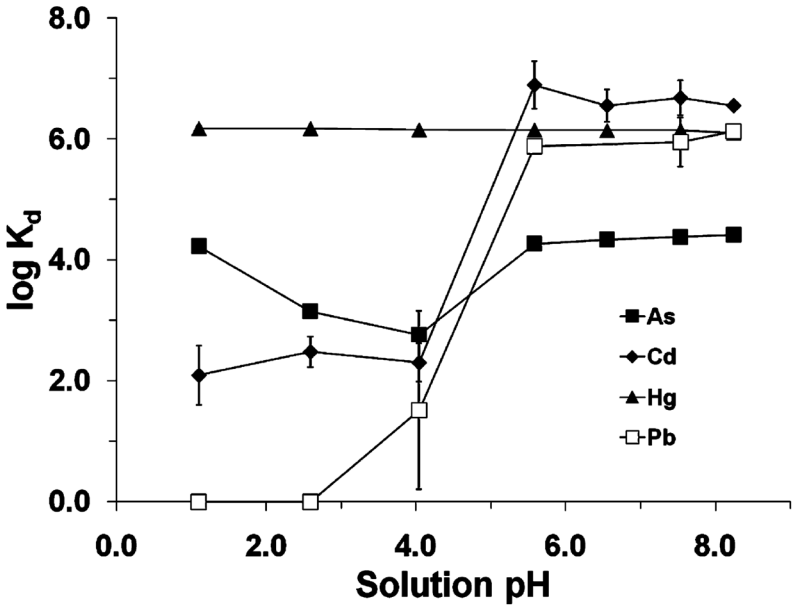

FIGURE 2.

K_d of As, Cd, Hg, and Pb, measured on SH-SAMMS in synthetic gastrointestinal fluids prepared by adjusting SGF with 0.2 M $NaHCO_3$ to the desired pH. Initial metal ion concentration = 50 μg/L. S/L = 0.2 g/L. Error bars given represent standard deviations and, when not visible, indicate a variance of less than the data icon size.

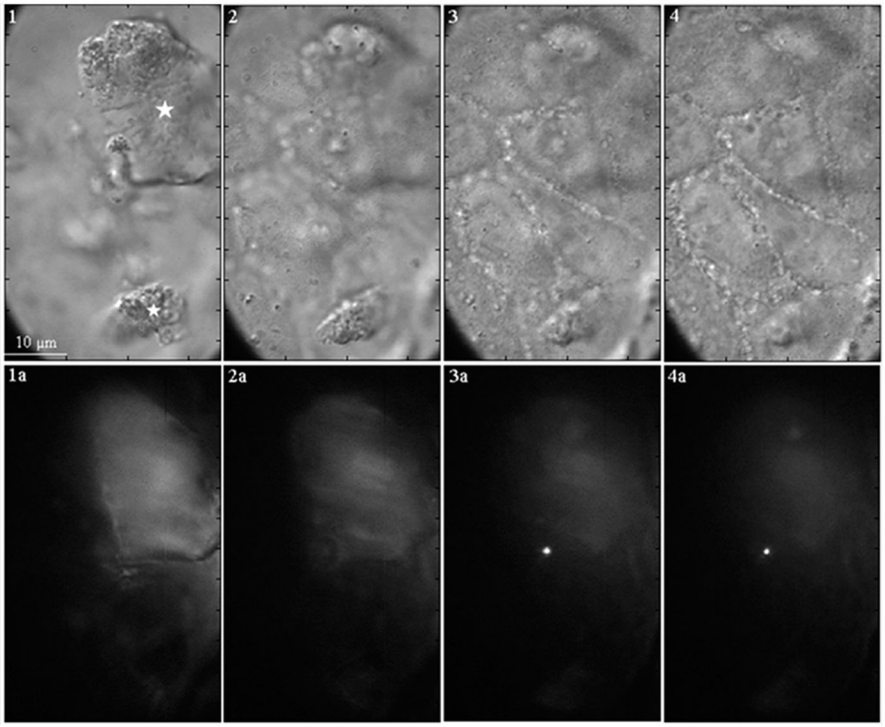

FIGURE 3.

DIC image (1) showing the presence of two large dye-tagged SAMMS particles (about 10 and 25 μm, indicated by the stars) on the cell surface. As images are taken deeper in the cells (2–4), the particles disappear. The correlated fluorescence image (1a and 2a) shows dim or no fluorescence signals from the dye-tagged particles as a result of fluorescence quenching by Trypan Blue. Together, these observations indicate that the large particles stay at the cell surface. The fluorescence images that are taken deeper in the cells (3a and 4a) show the presence of a bright spot, which indicates that a small particle (~1–2 μm) was internalized into the cytoplasm, where it was protected from the quenching by Trypan Blue.

Table 1

Sorbent Properties (Values Given for Functionalized Materials)

sorbent	pore size (nm)	surface area (m^2/g)	ligands/nm^2
SH-SAMMS (large pore)[a]	6.5	683	1.9
SH-SAMMS[b]	3.8	438	3.9
IDAA-SAMMS[c]	2.7	529	0.83
AcPhos-SAMMS[c]	2.2	480	1.1
Gly-Ur-SAMMS[c]	2.2	725	0.80
activated carbon	1.7	1445	N/A

[a] Unfunctionalized large-pore silica had a surface area of ~1000 m^2/g and a pore size of ~7.5 nm.

[b] Unfunctionalized silica had a surface area of ~870 m^2/g and a pore size of ~5.0 nm.

[c] Unfunctionalized silica had a surface area of ~750 m^2/g and a pore size of ~3.2 nm.

Table 2

Affinity (K_d) of As, Cd, Hg, and Pb for Various Sorbents in Blood[b]

	K_d (mL/g) in blood			
sorbent[a]	**As**	**Cd**	**Hg**	**Pb**
SH-SAMMS	4200	2000	1200	1300
EDTA-SAMMS	13	370	81	460
AcPhos-SAMMS	15	0	0	11
Gly-Ur-SAMMS	0	0	0	0
IDAA resin	0	450	36	2300
SH resin	38	0	0	0
activated carbon	9	0	0	1100

[a] Pore sizes are presented in Table 1.

[b] Measured at an initial metal concentration of 50 μg/L (each), S/L of 1 g/L, pH 7.5.

Table 3

Affinity (K_d) of As, Cd, Hg, and Pb for Various Sorbents in Urine[b]

	K_d (mL/g) in urine			
sorbent[a]	**As**	**Cd**	**Hg**	**Pb**
SH-SAMMS	3500	11000	5600	1900
EDTA-SAMMS	0	20000	1500	1200
AcPhos-SAMMS	46	220	160	130
Gly-Ur-SAMMS	0	12	200	26
IDAA resin	0	37000	180	7200
SH resin	80	3200	720	2400
activated carbon	150	5000	5200	12000

[a] Pore sizes are presented in Table 1.

[b] Measured at an initial metal concentration of 50 μg/L (each), S/L of 1 g/L, pH 6.92.

Table 4

Affinity (K_d) of SH-SAMMS for As, Cd, Hg, and Pb in Various Fluids[b]

				K_d (mL/g) in various matrices			
matrix[a]	**conductivity (mS/cm)**	**pH**	**available protein content**	**As**	**Cd**	**Hg**	**Pb**
dilute urine (rat)	1.8	7.2	+		7.9×10^4	2.8×10^4	5.6×10^3
whole human urine	7.9	6.9	++	3.5×10^3	1.1×10^4	5.6×10^3	1.9×10^3
whole human urine (large pore)	7.9	6.9	++	5.0×10^3	1.0×10^4	2.3×10^4	1.1×10^3
whole human blood	4.0	7.5	+++	4.2×10^3	2.0×10^3	1.2×10^3	1.3×10^3
whole human blood (large pore)	4.0	7.5	+++	4.2×10^3	3.3×10^3	7.6×10^3	1.9×10^3
SGF[c] (large pore)	32.9	1.1	−	1.7×10^4	1.7×10^2	1.5×10^6	0
SIF[d] (large pore)	5.9	6.8	−	2.7×10^4	7.7×10^5	2.7×10^5	2.0×10^4

[a] Silica pore sizes noted in Table 1.

[b] Measured at an initial metal concentration of 50 μg/L (each), S/L of 0.2 g/L except for urine, blood, and plasma, S/L of 1 g/L.

[c] SGF = synthetic gastric fluid.

[d] SIF = synthetic intestinal fluid.

ACS Appl Mater Interfaces. Author manuscript; available in PMC 2012 August 28.

Table 5

Maximum Capacity of Metal Uptake by SH-SAMMS As Predicted by the Langmuir Sorption Isotherm Model[a]

metal	max capacity (mg/g)	matrix[b]
Hg	380	SGF
Cd	50	SIF
As	8.5	SGF
As	29	SIF, RT
As	28	SIF, 37 °C

[a] All fits with regression better that 0.99.

[b] SGF (pH 1.11) contained 0.03 M NaCl, 0.085 M HCl, and 0.32% (w/v) pepsin; SIF contained 0.05 M KH_2PO_4. The pH was adjusted to 6.8 with 0.2 M NaOH.

Table 6

Uptake Study of Metal-Bound SH-SAMMS with a Caco-2 Cell Monolayer

sample	As^{III}	Cd^{II}	Hg^{II}	Pb^{II}	TEER (Ω cm^2)
metal-bound SAMMS (μg)[a]	1.4 ± 0.03	2.5 ± 0.00	2.5 ± 0.00	2.5 ± 0.00	
test group (ng)[b]	1.2 ± 0.01	0.3 ± 0.11	1.3 ± 0.43	0.5 ± 0.16	798 ± 16
blank (ng)[c]	2.1 ± 0.15	0.4 ± 0.12	0.9 ± 0.00	0.1 ± 0.03	792 ± 19
% metal transport	0	0	0.02	0.02	

[a]Estimated from 0.0025 g of SH-SAMMS bound with 0.6 mg of As and 1.0 mg of Cd, Hg, and Pb per g of SH-SAMMS.

[b]Metals in the basolateral side of Caco-2 cells after 2 h of contact with the material in footnote a, in triplicate.

[c]Metals in the basolateral side of Caco-2 cells after 2 h of contact with the filtrate of metal-bound SAMMS suspension (after solid removal), in duplicate.